Polymer 153 (2018) 538–547

Contents lists available at ScienceDirect

Polymer

journal homepage: www.elsevier.com/locate/polymer

Ionic liquid embedded polyimides with ultra-foldability, ultra-flexibility, ultra-processability and superior optical transparency

Ning-Bo Li, Meng Wang, Ling-Xiang Guo, Bao-Ping Lin, Hong Yang*

School of Chemistry and Chemical Engineering, Jiangsu Province Hi-Tech Key Laboratory for Bio-medical Research, Jiangsu Key Laboratory for Science and Application of Molecular Ferroelectrics, Southeast University, Nanjing, 211189, China

HIGHLIGHTS

- Ionic liquid/polyimide composites exhibit outstanding foldability, flexibility, processability and optical transparency.
- This 23-μm-thick polyimide composite film exhibits a high optical transmittance of 90.4% even at 450 nm wavelength and an incredibly low cutoff wavelength of 273 nm.
- This composite material has a super folding capability with a minimum bending radius of 1 μm, which is to our knowledge the lowest record for polymide materials.

ARTICLE INFO

Keywords:
Polyimide
Ionic liquid
Composite
Optical transparency
Flexibility

ABSTRACT

New generation spacecraft technology requires more and more deployable, light-weight, thin polymer films, in particular novel polyimide materials with high optical transparency, excellent foldability and superior flexibility. In this work, we develop a highly transparent, ultra-foldable, ultra-flexible and ultra-processable polyimide composite material by incorporating 5–8 wt% of ionic liquid 1-ethyl-3-methylimidazolium bis((trifluoromethyl) sulfonyl)imide into colorless polyimide matrices. This 23-μm-thick polyimide composite film exhibits a high optical transmittance of 90.4% even at 450 nm wavelength and an incredibly low cutoff wavelength of 273 nm. It is an extremely strong and flexible material, with a tensile modulus of 844.6 MPa, a tensile strength of 48.2 MPa, a high elongation at break of 108.4%, and an extraordinary minimum bend radius of 1 μm. It can be easily folded in half 4 times or twisted by 900° without any crack damages. Moreover, it has a low expense cost and good film processability for industrialization manufacturing. All of these superior performances render this ionic liquid/polyimide composite an ideal structural material for solar sails, solar arrays and thin-film photovoltaics, etc.

1. Introduction

With the rapid progress in space exploration technology, new-generation spacecrafts require more and more deployable, expandable structures, such as solar sails, solar arrays, thin-film photovoltaics, sunshields of space telescopes, etc. to save storage room and reduce launch costs [1,2]. As the fundamental part of such deployable structures, light-weight thin polymer films have drawn intense research efforts. Among them, polyimides (PIs), due to their excellent mechanical property, outstanding thermal stability and particularly high tolerance against space radiation [3–8], have been widely applied in space deployable structures, for example the basic structural material and the radiation shielding layers for solar sails and solar arrays. In such application scenarios, the ideal polyimide material must also possess high optical transparency, excellent foldability and flexibility, beyond its traditional technical performances.

Conventional PIs have strong absorption in the visible region and show characteristic orange/yellow color. In recent years, there have been many methods for development of colorless polyimides (CPIs), including the adoption of weak electron-accepting dianhydrides and/or electron-donating diamines, non-aromatic (cycloaliphatic) monomers, fluorinated substituents, the incorporation of kink linkages and pendant groups in the main chain to reduce linearity and molecular packing, as well as copolymerization strategy [9–17]. Although these methods have partly eliminated the electron transfer complexes and charge transfer (CT) interactions produced by the reaction of diamines and

* Corresponding author.
E-mail address: yangh@seu.edu.cn (H. Yang).

https://doi.org/10.1016/j.polymer.2018.08.048
Received 18 May 2018; Received in revised form 20 August 2018; Accepted 22 August 2018
Available online 27 August 2018
0032-3861/

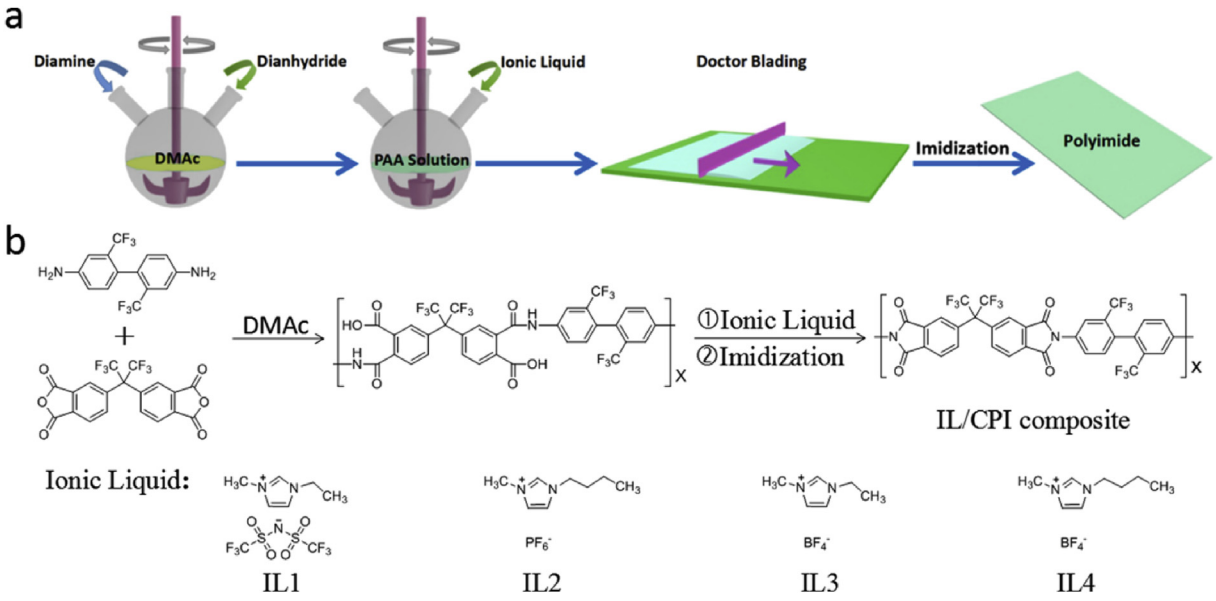

Fig. 1. a) Schematic diagram showing the preparation procedure of the ionic liquid embedded polyimide composite materials. b) Synthetic route of the ionic liquid embedded colorless polyimide composite materials.

dianhydrides, the enhanced optical transparencies of the resulting CPIs were still barely satisfactory [18–21].

On the other hand, increasing the optical transparency of CPI material is usually accompanied by the sacrifice of other performances, such as mechanical property, flexibility and processability, which severely limit its application as foldable, flexible substrates [22–26]. In order to solve these problems, many scientists have turned to develop PI composite materials by incorporating inorganic nanoparticles, such as nanoclays [27], inorganic silica [28], organosilicate [29], titanium dioxide [30,31], etc. Nevertheless, although these approaches have improved some properties of PIs, the desired perfect PI material with high optical transparency, excellent foldability and flexibility, considerable processability, outstanding thermal stability and superior mechanical property, is still under exploration.

In this work, we discover that incorporation of some specific ionic liquids (ILs) into PI matrices can dramatically improve the optical transparency, flexibility, foldability and processability of PI materials. ILs, as a class of liquid material composed of cation-anion pairs formed by the interaction of electrostatic coulombs, van-der-Waals forces and hydrogen bonds [32], have attracted intense scientific attention. In the view of their advantageous properties, including high thermal stability, non-flammability, low melting point, excellent solubilizing power, good chemical stability, and negligible vapor pressure [33], scientists have incorporated ILs into PI materials to prepare thin composite films for various applications, such as gas separation [34–37], polymer electrolyte fuel cells [38,39], printable polymer actuators [40], proton exchange membranes [41], etc. Although the roles of ILs in enhancing conductivity [42], decreasing the friction coefficient [43], acting as surfactants [44], catalyzing polyimidization reaction [45] of PIs have been investigated, there was barely any report studying the connections and influence rules between ILs and light transparency, flexibility, foldability and processability of IL/PI composites, which are on the contrary the main research contents of this paper.

2. Experimental

2.1. Materials

2,2′-Bis(trifluoromethyl)benzidine (TFB) and 4,4'-(hexafluoroisopropylidene)diphthalic anhydride (6FDA) were purchased from Bide Pharmatech Ltd, China. 1-Ethyl-3-methylimidazolium bis ((trifluoromethyl)sulfonyl)imide (IL1, 97% purity), 1-butyl-3-methylimidazolium hexafluorophosphate (IL2, 99% purity), 1-ethyl-3-methylimidazolium tetrafluoroborate (IL3, 98% purity), 1-butyl-3-methylimidazolium tetrafluoroborate (IL4, 99% purity), 3,5-diaminobenzoic acid (DABA), 4,4′-oxydianiline (ODA), and pyromellitic dianhydride (PMDA) were purchased from Aladdin Reagent Co., Ltd. 1,2,3,4-Cyclopentanetetracarboxylic dianhydride (CPDA) was purchased from TCI Development Co., Ltd, Shanghai. Dimethylacetamide (DMAc) was purified by distillation under reduced pressure over CaH_2 and stored over 4 Å molecular sieves. Other solvents and regents were used as received.

2.2. Synthesis of polyimides

The polyimides were synthesized by the conventional two-step procedure via poly(amic acid) precursors, followed by thermally curing at elevated temperatures. The polymerization of CPI (TFB/6FDA) is described herein as an example. First, TFB (0.87 g, 2.72 mmol) was dissolved in anhydrous DMAc (20 mL), ice-cooled and vigorously stirred to form a homogeneous transparent solution, to which an equimolar amount of 6FDA (1.21 g, 2.72 mmol) was added. The resulting solution was stirred vigorously at 0 °C for 2 h and stirred at room temperature for another 16 h to obtain a homogeneous viscous polyamic acid solution. The polyamic acid solution was coated on a glass substrate (10 cm long X 10 cm wide) by a doctor blade. Afterward, the polyamic acid sample was imidized to provide the final colorless polyimide by heat treatment, which was performed at 80 °C for 2 h, 110 °C for 2 h, 150 °C for 2 h, 170 °C for 2 h, 190 °C for 2 h, and 210 °C for 1 h, respectively. PI (Kapton) (ODA/PMDA), PI1 (DABA/6FDA) and PI2 (ODA/CPDA) were fabricated following the above protocol.

2.3. Synthesis of ionic liquid/polyimide

The fabrication of Ionic Liquid/Polyimide composite film is schematically illustrated in Fig. 1a. The synthesis process of the IL1/CPI composite material is described as an example, which is illustrated in Fig. 1b. First, TFB(0.87 g, 2.72 mmol) and 6FDA(1.21 g, 2.72 mmol) were polymerized to obtain 20.81 g of polyamic acid solution, following the above described synthetic protocol. Afterward, 1 wt%, 3 wt%, 5 wt %, 8 wt% or 10 wt% amount of ionic liquid IL1 (0.21 g, 0.64 g, 1.10 g, 1.81 g, 2.31 g, respectively) were added to the polyamic acid solution

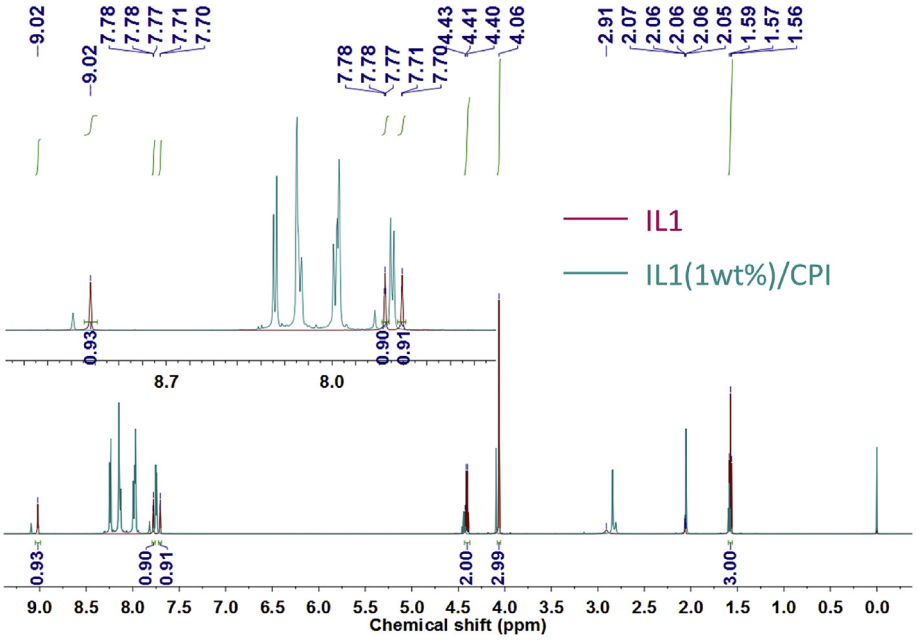

Fig. 2. ^{1}H NMR spectra of IL1 and IL1(1 wt%)/CPI composite film in Acetone-d6.

and stirred vigorously at room temperature for 6 h to obtain a more transparent and viscous solution. The solution was coated on a glass substrate (10 cm long X 10 cm wide) by a doctor blade and then thermally imidized as described above to obtain ionic liquid/colorless polyimide composites. IL1(1 wt%, 3 wt%, 5 wt%, 8 wt% or 10 wt%)/PI (Kapton), IL1(3 wt%, 5 wt%)/PI1 and IL1(3 wt%, 5 wt%)/PI2 were fabricated following the above protocol.

2.4. Characterization

^{1}H NMR spectra were recorded on a Bruker Avance III-HD 600 Spectrometer operating at 600 MHz in Acetone-*d6*. FTIR spectra were recorded on a Nicolet 5700 Fourier Infrared Spectrometer (Thermo Electron Scientific Instruments Corporation, America). The number average molecular weights (Mn) and polydispersity values (Mw/Mn) were determined by gel permeation chromatography (PL-GPC220, Agilent Technologies Inc., America) using THF as eluent at flow rate of 1.0 mL/min at room temperature. The UV–Vis spectrophotometer (UV2450, Shimadzu Corporation, Japan) was used to investigate the optical transmittance of CPIs, IL/CPI composites and Kapton. Combined multifunctional horizontal X-ray diffractometer (Rigaku Corporation, Japan) was used to investigate the morphological structure of CPIs and IL/CPIs. Tensile stress-strain curves of CPI and IL/CPI (180 mm long X 10 mm wide X 0.05 mm thick) samples were obtained on an Electromechanical Universal Testing Machine SANS E42.503 (Meters Industrial Co. Ltd, China) with a tensile rate of 5.0 mm/min at room temperature. Thermal gravimetric analysis (TGA) was performed with a TG209F3 (NETZSCH Instruments Co., Ltd, Germany) at a heating rate of 10 °C/min from 50 °C to 900 °C under nitrogen to examine the thermal stability of the prepared CPIs and IL/CPIs. Differential scanning calorimetry (DSC) of the CPIs and IL/CPIs composite films was analyzed using a differential scanning calorimeter (Q200; TA Instruments Co. Ltd, USA) under a nitrogen atmosphere. The samples were heated from 30 °C to 400 °C at a rate of 10 °C/min. After IL(8 wt%)/CPI film was bent, the edges of the film were pasted on a conductive tape. A scanning electron microscope (SEM, Phenom Scientific Instruments Co., Ltd, Netherlands) was applied to observe the morphology of the film surface and ultimately determine the minimum bending radius of the film.

3. Results and discussion

3.1. Preparation of ionic liquid/polyimide composite films

The fabrication procedure of the composite materials consisting of ILs and PIs is schematically illustrated in Fig. 1a. First, diamines and dianhydrides with equal molar equivalents were sequentially added in dimethylacetamide (DMAc) at 0 °C and stirred vigorously. A low reaction temperature and vigorous stirring were necessary to reduce the polycondensation rate and ensure the formation of a uniform viscous polyamic acid (PAA) solution. In the second stage of the process, ILs were added into the PAA solution, which became more and more viscous (Table S1). After 8 h vigorous stirring, the corresponding solution was coated onto a glass substrate by doctor blading. The final high-temperature thermal imidization process provided the IL/PI composite film.

To prepare optically transparent IL/CPI composite materials, we chose 2,2′-bis(trifluoromethyl)benzidine (TFB) and 4,4'-(hexafluoroisopropylidene)diphthalic anhydride (6FDA) as the diamine monomer and dianhydride monomer respectively (Fig. 1b). For comparison purpose, we applied 1-ethyl-3-methylimidazolium bis((trifluoromethyl)sulfonyl)imide (IL1), 1-butyl-3-methylimidazolium hexafluorophosphate (IL2), 1-ethyl-3-methylimidazolium tetrafluoroborate (IL3) and 1-butyl-3-methylimidazolium tetrafluoroborate (IL4) as the incorporated ILs, and prepared the corresponding IL/CPI composite films, named as IL1/CPI, IL2/CPI, IL3/CPI and IL4/CPI respectively.

The chemical structures of the fabricated CPI, IL/CPI composite films and the corresponding ILs were confirmed by ^{1}H NMR, FTIR and WXRD. The ^{1}H NMR spectra of CPI, IL1, IL2, IL3 and IL4 are included in Figures S1-S5. Fig. 2 presents the ^{1}H NMR spectra of IL1 and IL1 (1 wt %)/CPI composite film. Obviously, it was noted that the hydrogen of the imidazole ring underwent a downfield shift from δ ~9.02 ppm to δ ~9.09 ppm. The chemical shift variation suggested that IL1 and CPI backbones might form some hydrogen bonding interactions. Similarly, IL2, IL3, IL4 and CPI also presented such supramolecular interactions as shown in Fig S6-S8.

Fig. 3a presents the FTIR spectra of the pure IL1, pure CPI and various IL1/CPI composite films. ATR-IR peaks, such as 1786, 1784, 1725 cm^{-1} (C═O stretch), 1354 cm^{-1} (C—N stretch) and 1194, 1192, 1190, 1188 cm^{-1} (C—F stretch) ascribed to CPI molecules were

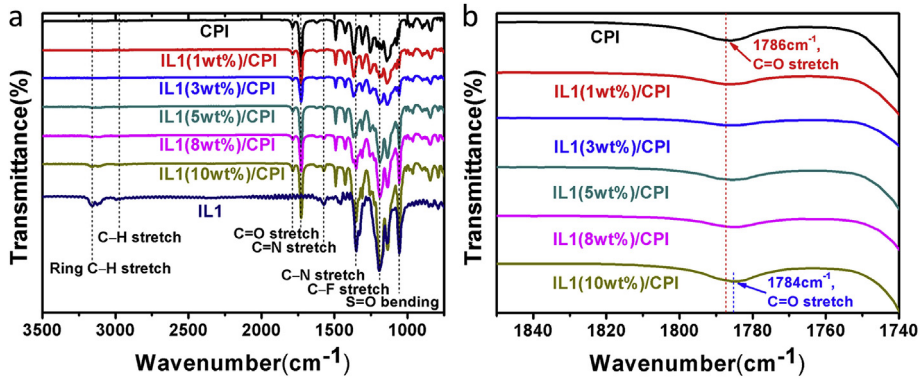

Fig. 3. a) FTIR spectra of pure IL1, pure CPI and various IL1/CPI composite films. b) FTIR spectra of pure CPI and various IL1/CPI composite films at 1850-1740 cm^{-1}.

observed on both sides of all the membranes. As to IL1, absorptions at 3200–3000 cm^{-1} (Ring C—H stretch), 3000–2900 cm^{-1} (C—H stretch), 1575 cm^{-1} (C═N stretch), 1192–1140 cm^{-1} (C—F stretch), and 1055 cm^{-1} (S═O bending) were observed on both sides of the composite membranes [25,34]. Fig. 3b shows the FTIR spectra of pure CPI and various IL1/CPI composite films recorded in the range of 1850–1740 cm^{-1}. It could be seen that the C═O stretching peak of CPI molecule shifted from 1786 cm^{-1} to 1784 cm^{-1} in IL1(10 wt%)/CPI composite film, which might also imply the existence of hydrogen bonds between the IL1 and CPI [46]. Similarly, Fig. S9 also indicates the possible existence of hydrogen bonds between IL2, IL3, IL4 and CPI chains, respectively. Fig. S10 shows the wide-angle X-ray diffraction (WAXD) patterns of pure PI and IL1/CPI samples. A characteristic broad amorphous halo of pure PI was observed in the range of 10°–30° (2θ) while IL1/CPI composite membranes were observed to have a wider halo in the range of 10°–40°. This amorphous and non-crystalline structure originated from the bulky $-CF_3$ group in the repeating unit of CPI, which was consistent to literature [25,47].

3.2. Optical properties of IL/CPI composite membranes

The optical transmittances of IL/CPI composite films were investigated by the ultraviolet–visible (UV–vis) spectrometer. As shown in Fig. 4a and b, compared with pure CPI sample, IL/CPI composites containing 3–5 wt% of IL2, IL3 or IL4 had much lower optical transmittances whereas IL1/CPI composite film increased the optical transparency and dramatically lowered the cutoff wavelength (absorption edge, λ_{cutoff}). Table 1 lists the cutoff wavelengths and the transmissions at 450 nm of all the examined films. IL1/CPI, CPI, IL3/CPI, IL2/CPI and IL4/CPI samples were ranked from the highest to lowest optical transmission. Apparently, the molecular structures of incorporated ILs markedly influenced the light transmittances of the corresponding IL/CPI composite films. From the perspective of molecular structure design, smaller sized cation 1-ethyl-3-methylimidazolium and larger sized anion bis((trifluoromethyl)sulfonyl)imide seemed to be superior to 1-butyl-3-methylimidazolium cation and hexafluorophosphate/tetrafluoroborate anions.

Thereafter, a series of IL1/CPI composite films with different composition ratios were further investigated, as shown in Figs. 4c and 5a. The highest transmittance of 90.2–90.4% at 450 nm and the lowest cutoff wavelength of 273 nm were achieved when the content of IL1 was in the range of 5–8 wt% (Table 1), further increase of IL1 content however weakened the optical transparency. Moreover, incorporation of IL1 into the classical Kapton material poly(4,4′-oxydiphenylene-pyromellitimide), could also dramatically enhance the optical transparency of Kapton membrane and significantly reduce its cut-off wavelength (Fig. 4d). As could be seen from Fig. 5b and Table S2, the IL1(5 wt%)/Kapton sample had the highest transparency, remarkably improved the pure Kapton transmittance of 76.0% at 550 nm to 84.8% and lowered the cutoff wavelength of Kapton from 411 nm to 373 nm. From the optical characteristics, it could be concluded that blending IL1 could significantly increase the optical transmittances of PI materials. This improvement might derive from the fact that in contrast to IL2, IL3 and IL4, the bis((trifluoromethyl)sulfonyl)imide anion of IL1 contained trifluoromethyl group, which could in some extent reduce linearity and molecular packing of PI main chains, thereby increase the light transmittance of PI material [9,48].

3.3. Mechanical and thermal properties of IL/CPI composite membranes

In addition to the optical property, mechanical property is another key consideration of IL/CPI composite material for deployable space structure application. Fig. 6 shows tensile stress-strain curves of the CPI and IL1/CPI composite films. The pure CPI sample had a high tensile modulus of 2929.6 MPa, a tensile strength of 67.4 MPa and an elongation at break of 2.9%. As long as the content of IL1 increased, the brittle CPI material became much tougher, the tensile modulus and tensile strength gradually decreased, accompanied by a significant increase in the elongation at break which benefited from the plasticizing effect of IL1. In addition, IL1 could be attached to the side chain of the polymer backbone by hydrogen bonding effect, resulting in excellent flexibility of the composite membranes [46,49]. As shown in Table 1, IL1(8 wt%)/CPI sample had a tensile modulus of 844.6 MPa, a tensile strength of 48.2 MPa and the highest elongation at break of 108.4% [50,51], which rendered CPI material superior flexibility. In addition, the tensile strengths of IL/CPI composites containing 3–5 wt% of IL2, IL3 or IL4 were lower than those of pure CPI, but their elongation at break values were higher than the one of pure CPI (Fig. S11). This might derive from the hydrogen bonding interaction between ILs and CPI, as well as the plasticizing effect of ILs.

To further examine the foldability of IL1/CPI material, we performed the bending test on pure CPI sample and IL1(8 wt%)/CPI composite film respectively. The schematic illustration (Fig. 7a) shows the calculation of the minimum bending radius of pure CPI sample and IL1(8 wt%)/CPI composite film. The minimum bending radius of the two films can be expressed as $r_1 = (d_1-d_2)/2$, where d_1 is the minimum bending distance of the film examined by a vernier caliper and d_2 is the thickness of the two layers after the film is folded 180°. Fig. 7b shows the minimum bending radius r_1 = 1920 μm of pure CPI film achieved at breaking, whereas IL1(8 wt%)/CPI composite membrane could be folded through completely 180° along fold line, indicating that the composite membrane had an excellent folding property. To accurately investigate the minimum bending radius of IL1(8 wt%)/CPI material, the edge of the bended composite membrane sample was adhered to a conductive tape which was then observed under scanning electron microscope (SEM), as schematically illustrated in Fig. 8a. The minimum

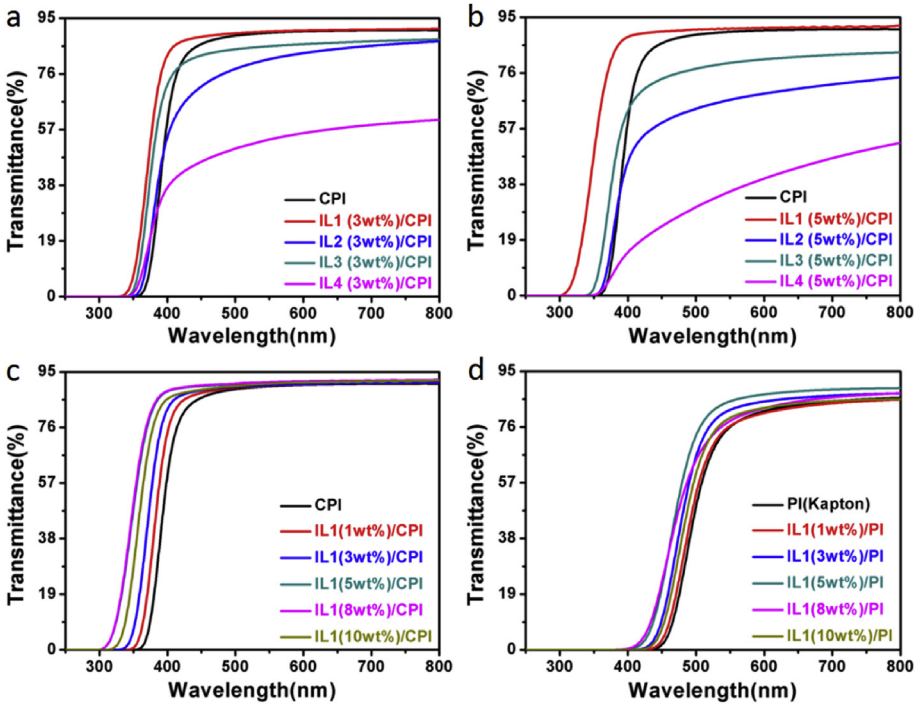

Fig. 4. Light transmittances of various IL/PI composite films: a) pure CPI and CPI composites containing 3 wt% of IL1, IL2, IL3 and IL4 respectively, b) pure CPI and CPI composites containing 5 wt% of IL1, IL2, IL3 and IL4 respectively, c) CPI composites containing 0 wt%, 1 wt%, 3 wt%, 5 wt%, 8 wt% and 10 wt% of IL1 respectively, d) PI (Kapton) composites containing 0 wt%, 1 wt%, 3 wt%, 5 wt%, 8 wt% and 10 wt% of IL1 respectively.

bending radius of the composite film can be expressed as $r_2 = d_3/2$, where d_3 is the minimum bending diameter of the composite film. Fig. 8b shows two SEM images of a composite film with a bending radius $r_2 = 6.0\,\mu m$. As could be seen from the images, there were no cracks at the bending regions of the composite films. When the bending radius was further shortened to 1.0 μm as shown in Fig. 8c, there were some tiny cracks appearing at the internal bending regions of the composite film, which concluded that the minimum bend radius of IL1(8 wt%)/CPI composite film was ca. 1.0 μm.

Fig. 9a and Movie S1 show that a pure CPI film was bent a certain angle and quickly broke into two parts, suggesting that this pure CPI film was hard and brittle. Fig. 9b and Movie S2 illustrate that IL1(8 wt%)/CPI composite film could be twisted by 900° and suffer no cracks or damages when recovered to its initial state. Fig. 9c and Movie S3 demonstrate that IL1(8 wt%)/CPI composite film, behaving like paper, could be folded in half four times reversibly [52]. It was further confirmed that embedding IL1 would empower CPI base material extraordinary mechanical flexibility, foldability and twistability.

Supplementary video related to this article can be found at https://doi.org/10.1016/j.polymer.2018.08.048.

The thermal gravimetric analyses (TGA) of IL1, pure CPI and IL1/CPI composite films with a heating rate of 10 °C/min under nitrogen atmosphere, were presented in Fig. 10. The TGA results were summarized in Table 1. The thermal decomposition temperatures (T_d) at 5% weight loss of IL1, pure CPI and a series of IL1/CPI composite materials were ranging from 381.5 to 528.3 °C. Compared with pure CPI sample, IL1/CPI composite films showed weakened thermal stabilities due to the presence of IL1 in the polymer matrix [34,49]. Interestingly, the thermal stabilities of IL1/CPI composite films were however higher than the one of IL1 molecule possibly due to the hydrogen bonding interaction of CPI and IL1 which would retard the thermal decomposition process of IL1 molecules [34,46]. In particular, the T_d at 5% weight loss of IL1(8 wt%)/CPI sample was 401.0 °C, indicating that IL1(8 wt%)/CPI sample had high thermal stability and could meet most

Table 1
Thickness, optical, mechanical and thermal property data of CPI and IL/CPI composite materials.

Film samples	Film thickness [μm]	$\lambda_{cut\text{-}off}$ [nm]	$T_{450\ nm}$ [%][a]	Td [°C][b]	TS [MPa][c]	TM [MPa][d]	EB [%][e]
CPI	28	350	86.2	528.3	67.4	2929.6	2.9
IL1(1 wt%)/CPI	26	339	87.8	414.8	70.7	1380.4	6.3
IL1(3 wt%)/CPI	27	321	88.7	392.6	59.5	1175.0	9.9
IL1(5 wt%)/CPI	24	273	90.2	398.4	44.7	1538.5	28.5
IL1(8 wt%)/CPI	23	273	90.4	401.0	48.2	844.6	108.4
IL1(10 wt%)/CPI	24	289	89.0	398.1	22.9	427.2	108.0
IL2(3 wt%)/CPI	27	344	71.7	-[f]	43.7	1348.9	3.2
IL2(5 wt%)/CPI	26	345	59.0	-[f]	50.8	1039.3	5.5
IL3(3 wt%)/CPI	25	333	82.4	-[f]	56.0	1476.0	5.9
IL3(5 wt%)/CPI	29	332	74.0	-[f]	30.2	1138.4	4.7
IL4(3 wt%)/CPI	25	335	46.1	-[f]	54.3	1120.4	7.3
IL4(5 wt%)/CPI	25	341	23.7	-[f]	44.7	1199.4	6.3

[a] Light transmittance measured at 450 nm.
[b] The thermal decomposition temperature at 5% weight loss.
[c] Tensile strength.
[d] Tensile modulus.
[e] Elongation at break.
[f] Data were not measured.

Fig. 5. Photograph images of a) various IL/CPI composite films containing 0–10 wt% of IL1 and b) various IL/Kapton composite films containing 0–10 wt% of IL1.

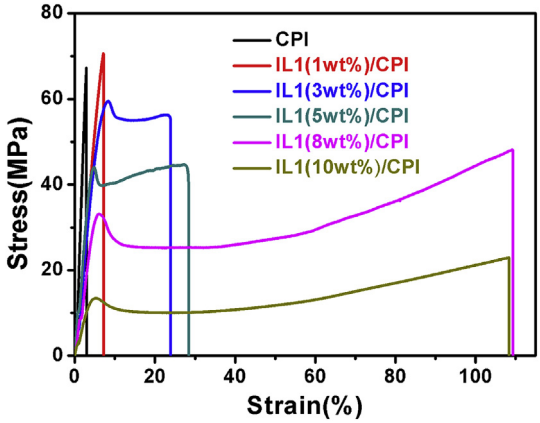

Fig. 6. Tensile stress-strain curves of pure CPI and various IL1/CPI composite films.

of the application requirements of colorless polyimides.

Fig. S12 presents the differential scanning calorimetry (DSC) curves of pure CPI and IL1/CPI composite films with a heating rate of 10 °C/min under nitrogen atmosphere. The glass transition temperature (T_g) of pure CPI and a series of IL1/CPI composite films were ranging from 75.6 to 332.2 °C. The T_g values of IL1/CPI composite films were apparently lower than the one of pure CPI due to the plasticizing effect of IL1, which would reduce the rigidity and brittleness of the polymer chains, resulting in softening of the polymer matrix [43,49].

3.4. Processability of composite membranes

In addition to the excellent optical, mechanical and thermal performances of IL/CPI composite membranes, the film manufacturing cost and processability are determining factors for industrialization production. The CPI films reported above were polymerized from two low-cost reagents 2,2′-dis(trifluoromethyl)benzidine (TFB) and 4,4'-(hexafluoroisopropylidene)diphthalic anhydride (6FDA). The commercial expense of 1-ethyl-3-methylimidazolium bis((trifluoromethyl)sulfonyl) imide (IL1) used in this work was also very low, which brought IL1/CPI composite material a prosperous industrialization potential.

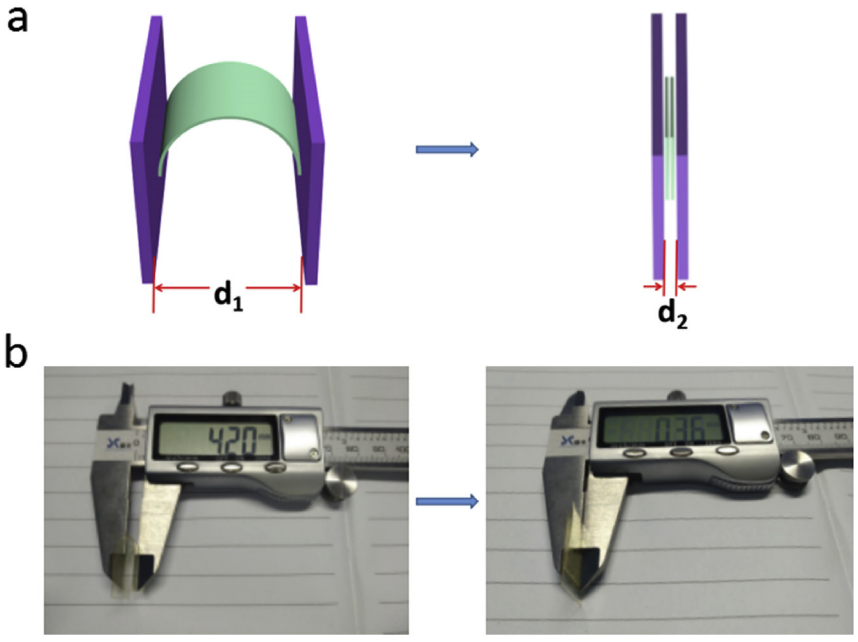

Fig. 7. a) Schematic illustration of the bending test. b) Photograph images of a pure CPI film bending examined by a vernier caliper.

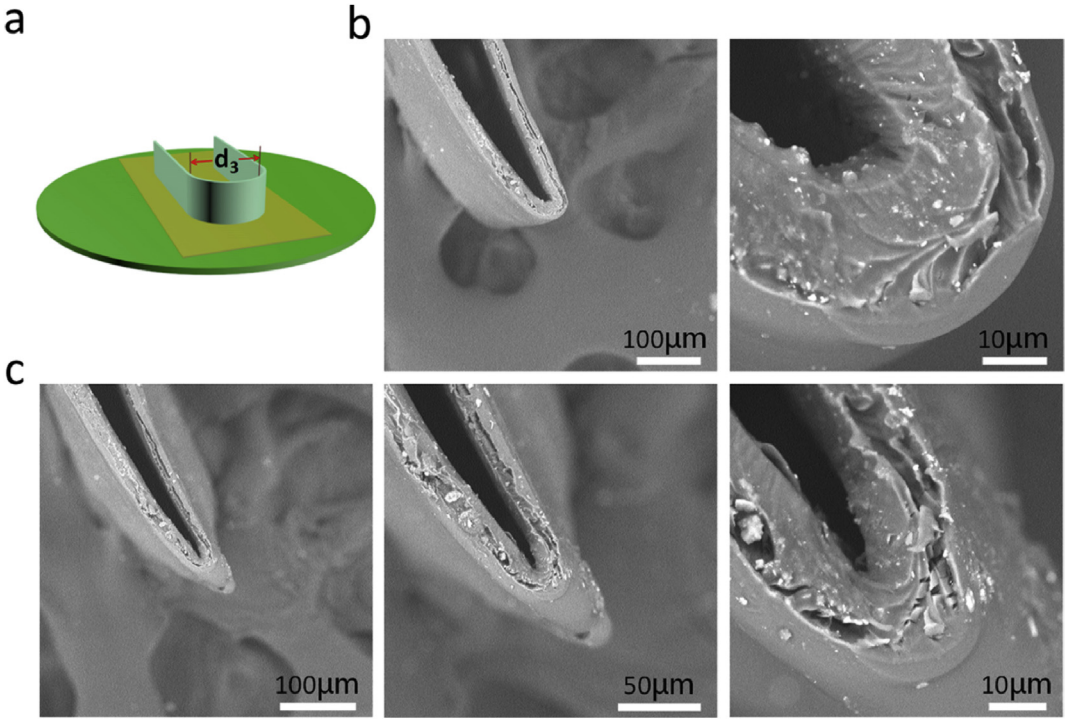

Fig. 8. a) Schematic illustration of IL1(8 wt%)/CPI composite bending test experiment. b) SEM images of the composite film bent with a bending radius of ca. 6.0 μm c) SEM images of the composite film bent with a bending radius of ca. 1.0 μm.

To examine the processability of IL1/CPI materials, we further tried to embed IL1 into two literature reported polyimide materials PI1 and PI2 which had poor processabilities and were difficult to form intact membranes [53,54]. As shown in Fig. 11a, PI1 was obtained by polymerization of 3,5-diaminobenzoic acid (DABA) and 4,4'-(hexafluoroisopropylidene)diphthalic anhydride (6FDA), PI2 was obtained by polymerization of 4,4′-oxydianiline (ODA) and 1,2,3,4-cyclopentanetetra-carboxylic dianhydride (CPDA). Traditionally, the content of diamine and dianhydride reactants in the reaction solvents should be in the range of 10–20 wt%, to form good-quality membranes through the solution casting method. Dilute polyamic acid solutions would result in broken PI films or even powder products. For example, as shown in Fig. 11b, when the content of diamine and dianhydride reactants in reaction solvents were lowered to 8.5 wt%, pure CPI sample was unable to form membranes. Following literature protocols [53,54], we also set the contents of diamine/dianhydride components of PI1 and PI2

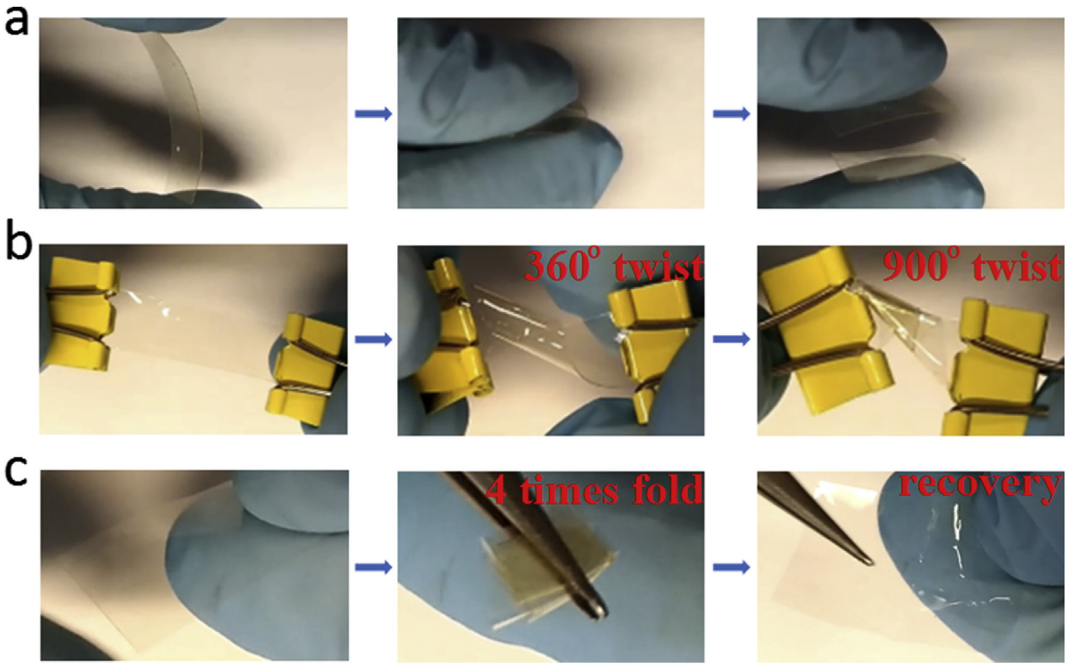

Fig. 9. a) A piece of pure CPI film is forced to bend and easily breaks into two parts. Supplementary Movie S1 shows this scenario. b) A piece of IL1(8 wt%)/CPI composite film is twisted by 900° and recovered to its initial status. Supplementary Movie S2 shows this scenario. c) A piece of IL1(8 wt%)/CPI composite film is folded in half 4 times and recovered to its initial state easily. Supplementary Movie S3 shows this scenario.

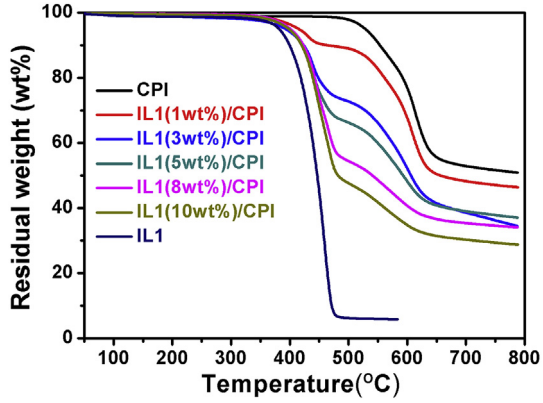

Fig. 10. Thermal gravimetric analysis curves of IL1, pure CPI and various IL1/CPI composite materials.

samples in reaction solvents as 12.5 wt% and 19.6 wt% respectively, which resulted in poor-quality membranes. However, after blending 3 wt% or 5 wt% of IL1 into polyimide matrices, CPI, PI1 and PI2 samples could not only form good-quality films but also become more transparent, because of the extraordinary plasticizing effect of IL1. These results implied that incorporation of IL1 could make some brittle polyimide materials to form good quality membranes, increase the optical transparency of the membranes, and greatly improve the processability of brittle polyimide materials.

4. Conclusion

In conclusion, an IL/CPI composite material with high optical transmittance and high thermal stability was successfully prepared by incorporating 5–8 wt% of 1-ethyl-3-methylimidazolium bis((trifluoromethyl)sulfonyl)imide into colorless polyimide matrices. This composite material has a super folding capability with a minimum bending radius of 1 μm, which is to our knowledge the lowest record for polymide materials. It can be easily folded in half 4 times or twisted by 900° without any crack damages. Furthermore, this IL/CPI composite has a low manufacturing cost, simple operation conditions and excellent processability, making it possible for large-scale industrial production, and ultimately widely used in spacecraft structural materials for solar sails, solar arrays and thin-film photovoltaics, etc.

The extraordinary foldability, flexibility and processability properties of this novel IL/CPI composite material might derive from the plasticizing effect of ionic liquids, as well as the contribution of the hydrogen bonding forces between ionic liquids and polyimide backbones. However, the scientific reason behind the fact that 1-ethyl-3-methylimidazolium bis((trifluoromethyl)sulfonyl)imide can greatly

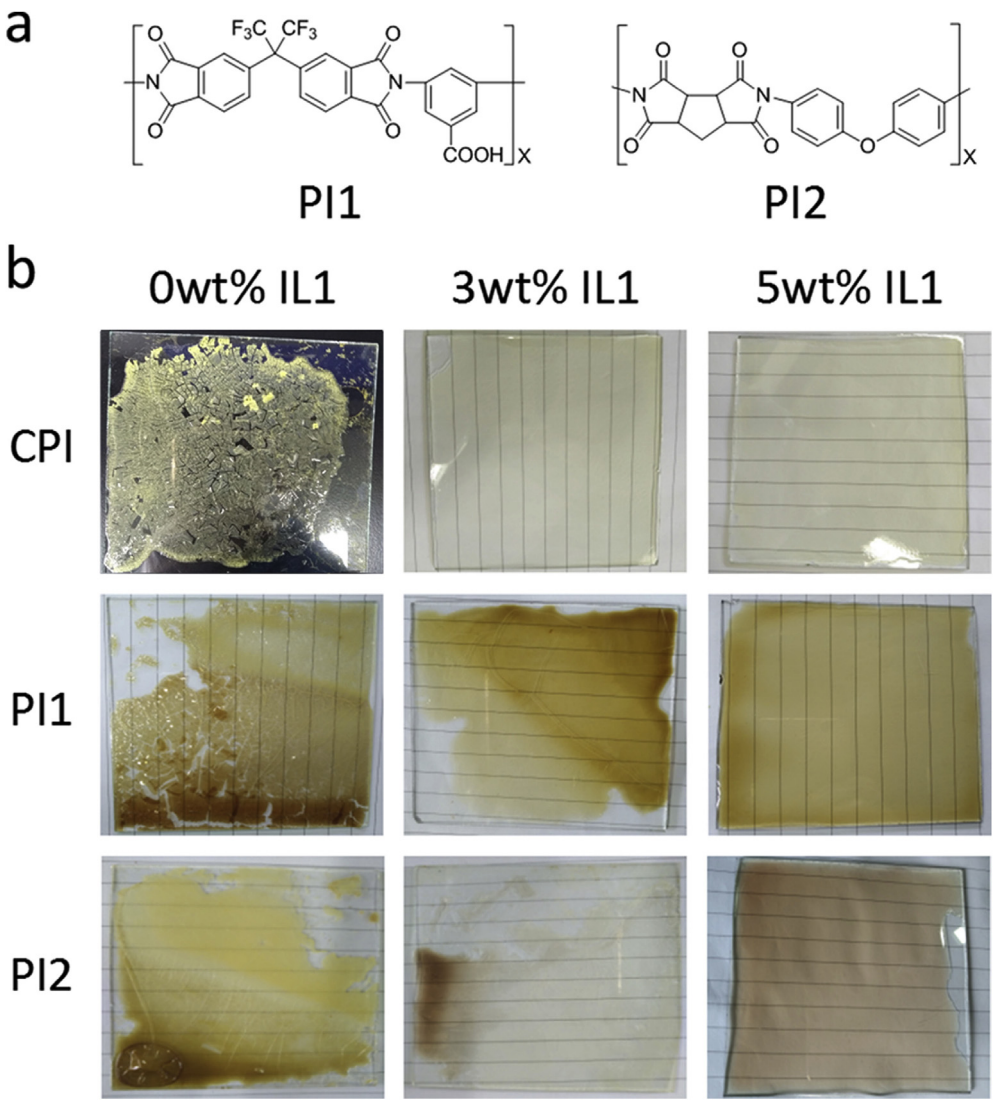

Fig. 11. a) Chemical structures of PI1 and PI2. b) Photograph images of CPI, PI1 and PI2 incorporated with different amounts of IL1.

improve the optical transmittance of polyimides whereas some other ionic liquids do weaken the transparency, is still under investigation.

Acknowledgements

This research was supported by National Natural Science Foundation of China (No. 21374016), Jiangsu Provincial Natural Science Foundation of China (BK20170024), and the Open Research Fund of State Key Laboratory of Bioelectronics, Southeast University.

Appendix A. Supplementary data

Supplementary data related to this article can be found at https://doi.org/10.1016/j.polymer.2018.08.048.

References

[1] P. Seefeldt, P. Spietz, T. Sproewitz, J.T. Grundmann, M. Hillebrandt, C. Hobbie, M. Ruffer, M. Straubel, N. Toth, M. Zander, Gossamer-1: mission concept and technology for a controlled deployment of gossamer spacecraft, Adv. Space Res. 59 (2017) 434–456.
[2] J. Block, M. Straubel, M. Wiedemann, Ultralight deployable booms for solar sails and other large gossamer structures in space, Acta Astronaut. 68 (2011) 984–992.
[3] E.N. Popova, V.E. Yudin, L.A. Myagkova, N.V. Kukarkina, M. Ya Goikhman, V.M. Svetlichnyi, Thermal aging of carbon-and glass-reinforced plastics based on heat-resistant polyimide binders, Russ. J. Appl. Chem. 82 (2009) 889–893.
[4] P. Thiruvasagam, Synthesis and characterization of AB-type monomers and polyimides: a review, Des. Monomers Polym. 16 (2013) 197–221.
[5] H. Shi, Y. Li, T. Guo, In situ preparation of transparent polyimide nanocomposite with a small load of graphene oxide, J. Appl. Polym. Sci. 128 (2013) 3163–3169.
[6] Y. Guan, C. Wang, D. Wang, G. Dang, C. Chen, H. Zhou, High transparent polyimides containing pyridine and biphenyl units: synthesis, thermal, mechanical, crystal and optical properties, Polymer 62 (2015) 1–10.
[7] H. Ni, J. Liu, Z. Wang, S. Yang, A review on colorless and optically transparent polyimide films: chemistry, process and engineering applications, J. Ind. Eng. Chem. 28 (2015) 16–27.
[8] C.L. Tsai, H.J. Yen, G.S. Liou, Highly transparent polyimide hybrids for optoelectronic applications, React. Funct. Polym. 108 (2016) 2–30.
[9] I.H. Choi, B. Sohn, J.H. Chang, Synthesis and characterization of transparent copolyimide films containing CF_3 groups: comparison with copolyimide nanocomposites, Appl. Clay Sci. 48 (2010) 117–126.
[10] M. Hasegawa, D. Hirano, M. Fujii, M. Hage, E. Takezawa, S. Yamaguchi, A. Ishikawa, T. Kagayama, Solution-processable colorless polyimides derived from hydrogenated pyromellitic dianhydride with controlled steric structure, J. Polym. Sci., Part A: Polym. Chem. 51 (2013) 575–592.
[11] M. Hasegawa, K. Kasamatsu, K. Koseki, Colorless poly (esterimide) s derived from hydrogenated trimellitic anhydride, Eur. Polym. J. 48 (2012) 483–498.
[12] M. Hasegawa, T. Ishigami, J. Ishii, K. Sugiura, M. Fujii, Solution-processable transparent polyimides with low coefficients of thermal expansion and self-orientation behavior induced by solution casting, Eur. Polym. J. 49 (2013) 3657–3672.
[13] C.H. Choi, B.H. Sohn, J.H. Chang, Colorless and transparent polyimide nanocomposites: comparison of the properties of homo-and co-polymers, J. Ind. Eng. Chem. 19 (2013) 1593–1599.
[14] J.C. Kim, J.H. Chang, Quaternary copolyimides with various monomer contents: thermal property and optical transparency, Macromol. Res. 22 (2014) 1178–1182.
[15] Y. Zhou, G. Chen, W. Wang, L. Wei, Q. Zhang, L. Song, X. Fang, Synthesis and characterization of transparent polyimides derived from ester-containing dianhydrides with different electron affinities, RSC Adv. 5 (2015) 79207–79215.
[16] H. Yeo, M. Goh, B.C. Ku, N.H. You, Synthesis and characterization of highly-fluorinated colorless polyimides derived from 4, 4'-((perfluoro-[1, 1'-biphenyl]-4, 4'-diyl) bis (oxy)) bis (2, 6-dimethylaniline) and aromatic dianhydrides, Polymer 76 (2015) 280–286.
[17] J.A. Spechler, T.W. Koh, J.T. Herb, B.P. Rand, C.B. Arnold, A transparent, smooth, thermally robust, conductive polyimide for flexible electronics, Adv. Funct. Mater. 25 (2015) 7428–7434.
[18] T. Maegawa, O. Miyashita, Y. Irie, H. Imoto, K. Naka, Synthesis and properties of polyimides containing hexaisobutyl-substituted T8 cages in their main chains, RSC Adv. 6 (2016) 31751–31757.
[19] K.H. Nam, S. Kim, J. Song, S. Baek, S.H. Paek, B.C. Ku, H. Han, Dimensionally stable and light-colored polyimide hybrid reinforced with layered silicate, Macromol. Res. 24 (2016) 104–113.
[20] Y. Zhou, G. Chen, H. Zhao, L. Song, X. Fang, Synthesis and properties of transparent polyimides derived from trans-1, 4-bis (2, 3-dicarboxyphenoxy) cyclohexane dianhydride, RSC Adv. 5 (2015) 53926–53934.
[21] T.T. Huang, C.L. Tsai, S. Tateyama, T. Kaneko, G.S. Liou, Highly transparent and flexible bio-based polyimide/TiO_2 and ZrO_2 hybrid films with tunable refractive index, Abbe number, and memory properties, Nanoscale 8 (2016) 12793–12802.
[22] I.H. Tseng, Y.F. Liao, J.C. Chiang, M.H. Tsai, Transparent polyimide/graphene oxide nanocomposite with improved moisture barrier property, Mater. Chem. Phys. 136 (2012) 247–253.
[23] M.H. Tsai, I.H. Tseng, S.L. Huang, C.W. Hsieh, Enhancement of dimensional stability and optical transparency of colorless organo-soluble polyimide by incorporation of silica and cosolvent, Int. J. Polym. Mater. Po. 63 (2014) 48–56.
[24] G. Chen, X. Pei, J. Liu, X. Fang, Synthesis and properties of transparent polyimides derived from trans-and cis-1, 4-bis (3, 4-dicarboxyphenoxy) cyclohexane dianhydrides, J. Polym. Res. 20 (2013) 159.
[25] K.H. Nam, D. Kim, J. Seo, K. Seo, H. Han, Effect of tetrapod ZnO whiskers on the physical and moisture barrier properties of transparent polyimide/TZnO-W composite films, Macromol. Res. 22 (2014) 1243–1252.
[26] X. Wang, F. Liu, J. Lai, Z. Fu, X. You, Comparative investigations on the effects of pendent trifluoromethyl group to the properties of the polyimides containing diphenyl-substituted cyclopentyl Cardo-structure, J. Fluorine Chem. 164 (2014) 27–37.
[27] Y. Kim, J.H. Chang, J.C. Kim, Optically transparent and colorless polyimide hybrid films with various clay contents, Macromol. Res. 20 (2012) 1257–1263.
[28] S.K. Kim, X. Wang, S. Ando, X. Wang, Highly transparent triethoxysilane-terminated copolyimide and its SiO_2 composite with enhanced thermal stability and reduced thermal expansion, Eur. Polym. J. 64 (2015) 206–214.
[29] Y. Jung, S. Byun, S. Park, H. Lee, Polyimide-organosilicate hybrids with improved thermal and optical properties, ACS Appl. Mater. Interfaces 6 (2014) 6054–6061.
[30] Y.Y. Yu, W.C. Chien, T.H. Wu, H.H. Yu, Highly transparent polyimide/nanocrystalline-titania hybrid optical materials for antireflective applications, Thin Solid Films 520 (2011) 1495–1502.
[31] H.J. Yen, C.L. Tsai, P.H. Wang, J.J. Lin, G.S. Liou, Flexible, optically transparent, high refractive, and thermally stable polyimide-TiO_2 hybrids for anti-reflection coating, RSC Adv. 3 (2013) 17048–17056.
[32] R.L. Vekariya, A review of ionic liquids: applications towards catalytic organic transformations, J. Mol. Liq. 227 (2017) 44–60.
[33] Z.L. Xie, H.B. Xu, A. Geßner, M.U. Kumke, M. Priebe, K.M. Fromm, A. Taubert, A transparent, flexible, ion conductive, and luminescent PMMA ionogel based on a Pt/Eu bimetallic complex and the ionic liquid [Bmim][$N(Tf)_2$], J. Mater. Chem. 22 (2012) 8110–8116.
[34] S. Kanehashi, M. Kishida, T. Kidesaki, R. Shindo, S. Sato, T. Miyakoshi, K. Nagai, CO_2 separation properties of a glassy aromatic polyimide composite membranes containing high-content 1-butyl-3-methylimidazolium bis (trifluoromethylsulfonyl) imide ionic liquid, J. Membr. Sci. 430 (2013) 211–222.
[35] P. Li, M.R. Coleman, Synthesis of room temperature ionic liquids based random copolyimides for gas separation applications, Eur. Polym. J. 49 (2013) 482–491.
[36] R. Shindo, M. Kishida, H. Sawa, T. Kidesaki, S. Sato, S. Kanehashi, K. Nagai, Characterization and gas permeation properties of polyimide/ZSM-5 zeolite composite membranes containing ionic liquid, J. Membr. Sci. 454 (2014) 330–338.
[37] M.S. Mittenthal, B.S. Flowers, J.E. Bara, J.W. Whitley, S.K. Spear, J.D. Roveda, D.A. Wallace, M.S. Shannon, R. Holler, R. Martens, Ionic polyimides: hybrid polymer architectures and composites with ionic liquids for advanced gas separation membranes, Ind. Eng. Chem. Res. 56 (2017) 5055–5069.
[38] S.Y. Lee, T. Yasuda, M. Watanabe, Fabrication of protic ionic liquid/sulfonated polyimide composite membranes for non-humidified fuel cells, J. Power Sources 195 (2010) 5909–5914.
[39] H. Deligöz, M. Yılmazoğlu, Development of a new highly conductive and thermomechanically stable complex membrane based on sulfonated polyimide/ionic liquid for high temperature anhydrous fuel cells, J. Power Sources 196 (2011) 3496–3502.
[40] S. Imaizumi, Y. Ohtsuki, T. Yasuda, H. Kokubo, M. Watanabe, Printable polymer actuators from ionic liquid, soluble polyimide, and ubiquitous carbon materials, ACS Appl. Mater. Interfaces 5 (2013) 6307–6315.
[41] B.K. Chen, T.Y. Wu, J.M. Wong, Y.M. Chang, H.F. Lee, W.Y. Huang, A.F. Chen, Highly sulfonated diamine synthesized polyimides and protic ionic liquid composite membranes improve PEM conductivity, Polymers 7 (2015) 1046–1065.
[42] E. Coletta, M.F. Toney, C.W. Frank, Effects of aromatic regularity on the structure and conductivity of polyimide-poly (ethylene glycol) materials doped with ionic liquid, J. Polym. Sci., Part B: Polym. Phys. 53 (2015) 509–521.
[43] M. Lv, F. Han, Q. Wang, T. Wang, Y. Liang, The structure properties and tribological behavior of the ionic liquid-polyimide composite films under high-vacuum environment, High Perform. Polym. 29 (2017) 170–177.
[44] H. Frank, U. Ziener, K. Landfester, Formation of polyimide nanoparticles in heterophase with an ionic liquid as continuous phase, Macromolecules 42 (2009) 7846–7853.
[45] M. Chen, S. Wang, Non-thermal polyimidization reaction using base-ionic liquid medium as a dual catalyst-solvent, RSC Adv. 6 (2016) 96914–96917.
[46] D.Y. Xing, S.Y. Chan, T.S. Chung, Fabrication of porous and interconnected PBI/P84 ultrafiltration membranes using [EMIM] OAc as the green solvent, Chem. Eng. Sci. 87 (2013) 194–203.
[47] C.H. Ju, J.C. Kim, J.H. Chang, Synthesis and characterization of colorless polyimide nanocomposite films, J. Appl. Polym. Sci. 106 (2007) 4192–4201.
[48] T. Xiao, X. Fan, D. Fan, L. Qiang, High thermal conductivity and low absorptivity/emissivity properties of transparent fluorinated polyimide films, Polym. Bull. 74 (2017) 4561–4575.
[49] H.A. Mannan, D.F. Mohshim, H. Mukhtar, T. Murugesan, Z. Man, M.A. Bustam, Synthesis, characterization, and CO_2 separation performance of polyether sulfone/[EMIM][Tf2N] ionic liquid-polymeric membranes (ILPMs), J. Ind. Eng. Chem. 54 (2017) 98–106.
[50] P.K. Tapaswi, M.C. Choi, Y.S. Jung, H.J. Cho, D.J. Seo, C.S. Ha, Synthesis and characterization of fully aliphatic polyimides from an aliphatic dianhydride with piperazine spacer for enhanced solubility, transparency, and low dielectric constant, J. Polym. Sci., Part A: Polym. Chem. 52 (2014) 2316–2328.
[51] J. Abraham, M.A.P.L. Kailas, N. Kalarikkal, S.C. George, S. Thomas, Developing

highly conducting and mechanically durable styrene butadiene rubber composites with tailored microstructural properties by a green approach using ionic liquid modified MWCNTs, RSC Adv. 6 (2016) 32493–32504.

[52] Y. Sun, R.B. Sills, X. Hu, Z.W. She, X. Xiao, H. Xu, W. Luo, H. Jin, Y. Xin, T. Li, Z. Zhang, J. Zhou, W. Cai, Y. Huang, Y. Cui, A bamboo-inspired nanostructure design for flexible, foldable, and twistable energy storage devices, Nano Lett. 15 (2015) 3899–3906.

[53] D.H. Wang, R.N. McKenzie, P.R. Buskohl, R.A. Vaia, L.S. Tan, Hygromorphic polymers: synthesis, retro-michael reaction, and humidity-driven actuation of ester-sulfonyl polyimides and thermally derived copolyimides, Macromolecules 49 (2016) 3286–3299.

[54] H.C. Yu, S.V. Kumar, J.H. Lee, S.Y. Oh, C.M. Chung, Preparation of robust, flexible, transparent films from partially aliphatic copolyimides, Macromol. Res. 23 (2015) 566–573.